How Can 5G Network Coverage be Optimized to Avoid Saturation in Security-Threatening Situations?

Mohamad Younes and Yves Louet

Abstract – This article studies the optimization of coverage within fifth-generation (5G) networks, characterized by a high density of base stations, particularly in crisis or security threat contexts. Our main objective was determining the most efficient transmission mode for delivering emergency alerts under varying conditions. To this end, we propose two promising solutions. The first is based on the joint use of the classic unicast transmission mode (UC) with beamforming (BF), while the second involves broadcast mode transmission via intercell cooperation, known as the single frequency network (SFN). We closely compared the performance of these modes with the UC mode, focusing on the evaluation of user coverage and the search for an optimal compromise between the coverage and key system parameters. In addition, our analysis focused on the search for system parameter thresholds, enabling us to determine the limit values beyond which the relative effectiveness of BF and SFN modes is reversed in terms of coverage probability. The results obtained in this study offer a promising contribution to combating the saturation of 5G networks in critical environments by effectively choosing the optimum transmission mode between UC, BF, and SFN to fully meet the requirements of modern communications.

1. Introduction

In recent years, mobile networks have experienced rapid technological growth, marked by an exponential increase in the number of users and the demand for data transfer [1, 2]. Mobile network technologies must constantly improve to meet these growing expectations, aiming to reduce latency, increase transmission speed, and increase overall capacity. The advent of fifth-generation (5G) mobile communications represents a major step forward in this trend, bringing substantial improvements. However, it is imperative to manage these advances intelligently, taking into account environmental constraints, spectrum limitations, necessary investments, and associated energy consumption, to ensure sustainable and efficient deployment [1–4].

Improving the performance of 5G technology has involved various techniques, including base station (BS) densification [2, 3], the use of massive antennas [4, 5], device-to-device communications [1], distributed antenna systems [6], the implementation of beamforming [4, 5], and the optimization of user equipment scheduling [7]. Despite these advances, guaranteeing optimal user coverage remains a major challenge to fully exploit the potential of 5G. In particular, rural areas and massive machine-type communications pose considerable coverage challenges. In addition, areas at cell boundaries encounter problems associated with uneven coverage and intercell interference. Careful coverage planning is, therefore, essential to avoid network outages [3, 5–7]. In this context, adopting network models based on the spatial distribution of BS according to the Poisson point process (PPP), rather than sticking to the classic hexagonal model, is proving unavoidable. This approach better reflects the complexity of 5G network deployments and produces results that are more relevant to real deployment scenarios [1, 4, 8].

Our study focused primarily on the challenges associated with coverage and interference management in 5G networks characterized by a high density of BS distributed according to PPP. These challenges are of particular importance in security threat scenarios, where BS must be able to effectively broadcast emergency messages to a wide audience. However, for a thorough understanding of network performance, studying its robustness is essential. This approach makes it possible to assess how performance evolves as a function of system parameters [9–11]. In this context, our analysis focused particularly on the robustness of different transmission modes regarding coverage in the face of system parameter variability and random BS localization.

When optimizing 5G coverage, the choice of transmission mode for signals emitted by BS is paramount, particularly in large-scale transmissions. The unicast mode (UC), traditionally predominant within cellular networks, is generally considered the standard for delivering personal content. This mode offers the flexibility to adapt the connection according to channel conditions, thus maximizing the data rate each user receives. However, its intensive use in scenarios where multiple users simultaneously request the same service can lead to inefficient management of radio resources [4]. The resulting interference can severely disrupt coverage, posing considerable problems for maintaining network performance.

Our study presents two effective solutions to meet these complex challenges. The first combines the UC transmission mode with beamforming (BF), while the second consists of broadcast mode transmission via intercell cooperation, also known as the single frequency network

Manuscript received 22 October 2023.

Mohamad Younes is with Research Center of the Military Academy of Saint-Cyr Coëtquidan, Guer 56381, France; e-mail: mohamad.younes@st-cyr.terre-net.defense.gouv.fr. Yves Louet is with IETR UMR CNRS 6164, CentraleSupélec at Rennes Campus, Cesson-Sévigné 35557, France; e-mail: yves.louet@centralesupelec.fr.

(SFN). This article builds on our previous work [12], where we conducted a comparative study between UC and SFN modes. Our results showed that SFN mode consistently outperformed conventional UC mode, regardless of the system parameters. However, in this paper, we explored the possibility that BF mode may outperform SFN broadcast mode in certain scenarios, notably by increasing the number of antennas per BS sector. Thus, this study made a significant contribution by assessing the usefulness of each mode in guaranteeing better coverage, particularly in crucial situations. In addition, our analysis focused on identifying thresholds associated with system parameters such as BS density, BS transmit power, and the number of antennas per sector. These thresholds delimit the levels beyond which relative efficiency, in terms of coverage probability, switches between BF and SFN modes. This research also enabled us to find an optimal compromise between the coverage offered to users and the system's main parameters. The results obtained in this study identified the optimum mode between UC, BF and SFN, thus reinforcing the resilience of wireless communications in the face of such demanding circumstances as those associated with crises and potential dangers. These results open up promising prospects for designing more efficient 5G telecommunications networks, offering better coverage thanks to selecting the most suitable mode.

2. System Model

In this study, we adopted a configuration where high-density BS was randomly distributed according to the PPP law. We assumed all BS were equipped with three sectors, each covering an angle of 120°. Signals were transmitted using orthogonal frequency division multiplexing technology in the various transmission modes while maintaining identical transmit power, carrier frequency, and bandwidth. This approach enabled us to make a fair comparison of performance between the two modes, maintaining constant conditions for all essential transmission parameters.

In our analysis, the signal power received by a user located at a distance $r_{g,i}$ from the base station (BS_i) was determined by several parameters. This included the path loss exponent α, the fading factor h_i, and the shadowing parameter e^{χ}, which are defined as follows:

$$P_{rx} = P_{tx}\kappa r_{g,i}^{-\alpha} e^{\chi} h_i G(\theta), \tag{1}$$

where P_{tx} is the transmission power of the BS, κ is the attenuation coefficient, and α is the path loss exponent. h_i is a randomly distributed exponential variable with a unit rate, χ is a normally distributed random variable with a mean of zero and a variance of σ^2, and $G(\theta)$ is the antenna gain calculated in the direction θ [13].

We modeled the shadowing phenomenon using a lognormal random variable, denoted e^{χ}, where χ is the sum of two components: $\chi = \chi_c + \chi_i$. The χ_c component takes into account obstacles close to the receiver, while χ_i takes into account independent obstacles for each BS. Shadowing is defined by its standard deviation of dispersion, denoted $\sigma = \frac{10}{\sigma_{dB} ln(10)}$, and the total variance can be expressed as $\sigma^2 = \sigma_c^2 + \sigma_i^2$. In the continuation of our analysis, we made the assumption that $\sigma_c^2 = \sigma_i^2 = \frac{\sigma^2}{2}$. Taking channel effects into account, we can describe the received signal power from the base station BS_i as follows:

$$P_{rx} = P_{tx}\kappa r_{g,i}^{-\alpha} e^{\chi_c} e^{\chi_i} h_i G(\theta) = P_{tx}\kappa r_i^{-\alpha} e^{\chi_c} h_i G(\theta), \tag{2}$$

where r_i is the adjusted distance between the user and the base station BS_i, taking into account the impact of the obstacle in the vicinity of BS_i (χ_i) on the actual distance between the user and BS_i ($r_{g,i}$). This distance adaptation, denoted $r_i = e^{-\frac{\chi_i}{\alpha}} r_{g,i}$, can be viewed as a modification of the initial position of BS_i.

3. Coverage Probability of Conventional UC Mode and Proposed Solutions

In this section of our study, we conducted a detailed comparison of coverage probability by examining the following three transmission modes: UC, BF, and SFN. The coverage probability (p_c) of each mode is defined as the probability that the signal-to-noise-plus-interference ratio (SINR) exceeds a predefined threshold, denoted S. This coverage probability is expressed as follows: $p_c = P\{\gamma \geq S\}$, where γ represents the SINR specific to the transmission mode in question. We then explored the calculation of the SINR γ for each of the modes between UC, BF and SFN.

In the UC mode, only the service BS (BS_s) provides useful signal power ($P_{s,UC}$), while all other BS generate interference. The received signal power ($P_{s,UC}$) is therefore calculated specifically for the service BS (BS_s), with the following notation: $P_{s,UC} = P_{tx}\kappa r_s^{-\alpha} e^{\chi_c} h_s G(\theta_{s,t})$, where the subscript s designates the service BS, while the subscript t designates the service sector of the service BS. As far as the interference power is concerned, it is divided into two parts. The first $I_{s,UC}$ relates to the interference sectors of the three-sector service BS. The second $I_{i\in\Psi/i\neq s,UC}$ is associated with the other BS present in the study area. Consequently, the SINR of a user served in UC mode is expressed as the ratio between the useful power received ($P_{s,UC}$) and the sum of the interference power ($I_r = I_{s,UC} + I_{i\in\Psi/i\neq s,UC}$) and the noise P_N as follows:

$$\gamma_{UC} = \frac{P_{s,UC}}{I_{s,UC} + I_{i\in\Psi/i\neq s,UC} + P_N}, \tag{3}$$

with,

$$I_{s,UC} = P_{tx}\kappa r_s^{-\alpha} e^{\chi_c} h_s \sum_{j=1/j\neq t}^{3} G(\theta_{s,j}), \tag{4}$$

$$I_{i\in\Psi/i\neq s,UC}=P_{tx}\kappa e^{\chi_c}\sum_{i\in\Psi/i\neq s}r_i^{-\alpha}h_i\sum_{j=1}^{3}G(\theta_{i,j}),\tag{5}$$

where index j denotes the interference sectors of the BS and index i denotes the interference-generating BS, and Ψ is the set of all BS distributed according to PPP.

Regarding BF mode, it's important to note that the BF technique uses an antenna array to increase beam gain in a certain direction. To implement the BF mode, we deployed a uniform linear array comprising N_a antennas per BS sector equipped with three sectors. As with UC mode, the expression for SINR in BF mode is formulated as follows:

$$\gamma_{BF}=\frac{P_{s,BF}}{I_{s,BF}+I_{i\in\Psi/i\neq s,BF}+P_N},\tag{6}$$

with,

$$P_{s,BF}=N_aP_{tx}\kappa r_s^{-\alpha}e^{\chi_c}h_iG(\theta_{s,t}),\tag{7}$$

$$I_{s,BF}=P_{tx}\kappa r_s^{-\alpha}e^{\chi_c}h_s\sum_{j=1/j\neq t}^{3}A\left(\theta_{s,j},\phi_{s,j}\right),\tag{8}$$

$$I_{i\in\Psi/i\neq s,BF}=P_{tx}\kappa e^{\chi_c}\sum_{i\in\Psi/i\neq s}r_i^{-\alpha}h_i\sum_{j=1}^{3}A\left(\theta_{i,j},\phi_{i,j}\right),\tag{9}$$

where $A(\theta,\phi)$ is the array gain for one sector in the θ direction calculated as follows [14]:

$$A(\theta,\phi)=\begin{cases}\dfrac{sin^2\left[N_a\frac{\pi}{2}(sin(\phi)-sin(\theta))\right]}{N_a sin^2\left[\frac{\pi}{2}(sin(\phi)-sin(\theta))\right]}, & \theta\neq\phi\\ N_aG(\theta), & \theta=\phi\end{cases},\tag{10}$$

where $-60^\circ\leq\theta\leq 60^\circ$. Note that antenna orientation was determined as a function of an orientation angle ϕ measured from the antenna's boresight axis.

Next, we focused on the cooperative intercell transmission in broadcast mode, using the SFN technique, which was introduced as part of the 3rd Generation Partnership Project (3GPP) by Release-9 LTE. This strategy relies on the synchronization of several transmitters, enabling them to broadcast the same content on an identical carrier frequency, thus favoring a constructive combination of the power received by the receiver. Within an SFN zone, all BS contributes to the received power (P_{SFN}) and also generates interference power (I_{SFN}) from delayed signals. For an SFN zone comprising a given number of BS participating in synchronized transmission (N_{BS}), the SINR in SFN mode is calculated as follows:

$$\gamma_{SFN}=\frac{P_{SFN}}{I_{SFN}+P_N},\tag{11}$$

with:

$$P_{SFN}=P_{tx}e^{\chi_c}\kappa\sum_{i=1}^{N_{BS}}\delta_i r_i^{-\alpha}h_i\sum_{j=1}^{3}G(\theta_{i,j}),\tag{12}$$

$$I_{SFN}=P_{tx}e^{\chi_c}\kappa\sum_{i=1}^{N_{BS}}(1-\delta_i)r_i^{-\alpha}h_i\sum_{j=1}^{3}G(\theta_{i,j}),\tag{13}$$

where δ_i is the weight function of the useful part of a signal received within the SFN zone [4].

4. Simulation Results and Discussion

The service area considered extends over 400 km^2 square, where the BS are distributed according to a PPP type random distribution with a specific density λ. Our simulations were performed in accordance with the parameters stated in the 3GPP standard [13], using the following values: $\kappa = 0.0295$, $\alpha = 3.76$, and $\sigma_{dB} = 10\ dB$. Finally, the δ_i function was calculated taking $T_g = 16.67\ \mu s$ and $T_u = 66.7\ \mu s$.

In this section, we carried out a comparative analysis of the coverage probability (p_c) between the different transmission modes, namely UC, BF, and SFN, with the aim of determining the optimum mode in various situations. To do this, we ran 10^4 Monte Carlo simulations, where a new random BS distribution was generated at each iteration. It is important to note that in all simulations, the BS transmits the same content in the different modes, at the same transmission power (P_{tx}), using the same carrier frequency ($f_c = 2\ GHz$) and bandwidth ($\omega = 5\ MHz$).

The results for coverage probability p_c for the different transmission modes are shown in Figure 1, highlighting the significant impact of BS location. This influence manifests itself in significant variations in p_c as a function of the target SINR (S), covering a range from $-5\ dB$ to $12\ dB$. It should be noted that the p_c analysis presented in Figure 1 takes into account different values of BS density ($\lambda_1 = 0.25\ BS/km^2$ and $\lambda_2 = 2\ BS/km^2$), as well as the number of antennas per sector in BF mode ($N_{a1}=2$ and $N_{a2}=8$), all while maintaining a constant transmission power of $0.5\ W$.

We now turn to a comparative analysis of p_c between UC, BF, and SFN modes. Figure 1 shows that, whatever the BS density scenario considered, UC mode offers the most limited coverage compared with the other modes. In contrast, the SFN mode offers the best coverage, reaching a rate of 100% when the BS density λ is equal to λ_2. It's also important to note that increasing the number of antennas per sector (N_a) in BF mode generates a significant gain in coverage compared with UC mode. For example, with a target SINR of $S = 2\ dB$ and a BS density of $\lambda=\lambda_1$, the coverage probability p_c increases

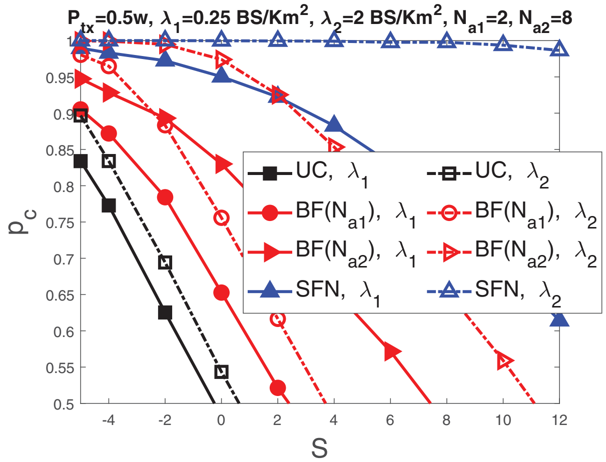

Figure 1. Coverage probability p_c in UC, BF, and SFN modes as a function of target SINR S, with $P_{tx} = 0.5\ W$ and different values λ and N_a.

from 37.46% (in UC mode) to 52.14% with $N_a = N_{a1}$ and continues to increase significantly to 74.96% with $N_a = N_{a2}$.

Regarding the impact of BS density, we observe a slight improvement in p_c in UC mode as the density increases from λ_1 to λ_2. However, this improvement remains limited due to the increase in interference resulting from the presence of a greater number of BS in the study area. Nevertheless, it is essential to note that a significant improvement in coverage was observed in both solutions implemented, particularly the BF and SFN modes. For example, when we compared the coverage probability for the two densities (with $S = 2\ dB$), we found that p_c reached 74.96% in BF mode with $N_a = N_{a2}$, while in SFN mode a rate of 92.24% was obtained at $\lambda = \lambda_1$. By increasing the density to λ_2, a clear improvement in p_c was observed, reaching 92.54% (in BF mode with $N_a = N_{a2}$) and 100% (in SFN mode).

Careful analysis of the BF and SFN mode coverage curves shown in Figure 1 for different values of N_a and λ reveals two clear intersections. The first occurs when the target SINR is $S = -2\ dB$, marking a critical transition point in BF mode performance. When S is below $-2\ dB$, the BF mode configured with the couple (N_{a1}, λ_2) outperforms the BF mode configured with (N_{a2}, λ_1). However, when S exceeds $-2\ dB$, the BF mode with (N_{a2}, λ_1) becomes more efficient than that with (N_{a1}, λ_2). The second intersection occurs between the BF and SFN mode curves when $S = +2\ dB$. Specifically, when S is less than $+2\ dB$, the BF mode with the couple (N_{a2}, λ_2) outperforms the SFN mode configured with λ_1, while when S exceeds $+2\ dB$, the SFN mode configured with λ_1 becomes more efficient than the BF mode configured with (N_{a2}, λ_2). These observations clearly demonstrate the effectiveness of each of the BF and SFN modes in significantly reducing total interference, which is particularly relevant in network saturation in crisis situations.

It is essential to remember that the coverage probability results p_c, obtained in Figure 1, were obtained with a transmission power (P_{tx}) of $0.5\ W$. To deepen our analysis, we examined the impact of P_{tx} by varying its value from $0.05\ W$ to $20\ W$ (Figure 2), while taking into account two BS densities ($\lambda_1 = 0.25\ BS/km^2$ and $\lambda_2 = 2\ BS/km^2$) and a fixed target SINR value ($S = 4\ dB$). Figure 2 shows, regardless of the value of P_{tx}, UC mode systematically presents the most limited coverage for the two BS densities studied. In contrast, the SFN mode offers the best coverage when $\lambda = \lambda_2$. However, it is interesting to note that intermediate coverages between the minimum and maximum values are obtained with the SFN mode for a density of $\lambda = \lambda_1$ and the BF mode for both densities. Specifically, an intersection between the BF and SFN mode curves occurs when $P_{tx} = 0.4\ W$. Consequently, when P_{tx} is less than $0.4\ W$, the BF mode configured with the couple $(N_a = 8, \lambda_2)$ outperforms the SFN mode with λ_1. On the other hand, when P_{tx} exceeds $0.4\ W$, the SFN mode with λ_1 becomes more efficient. In addition, Figure 2 provides relevant information regarding the minimum power required to achieve a predefined coverage. For example, to achieve 70% coverage, a minimum power of $0.1\ W$ would be required in SFN mode with λ_2, while in BF mode with λ_1, a minimum power of $0.8\ W$ would be required. To achieve 80% coverage, the minimum power required would be $0.08\ W$ in SFN mode with λ_2 and $0.3\ W$ in BF mode with λ_1. In summary, Figure 2 highlights the crucial importance of good transmission power matching, to meet coverage requirements and optimize system energy efficiency, depending on the chosen transmission mode.

5. Conclusion

In this article, we focused on optimizing the coverage of 5G networks, particularly in contexts exposed to security threats. With this in mind, our proposal of two transmission modes, namely UC mode with BF and

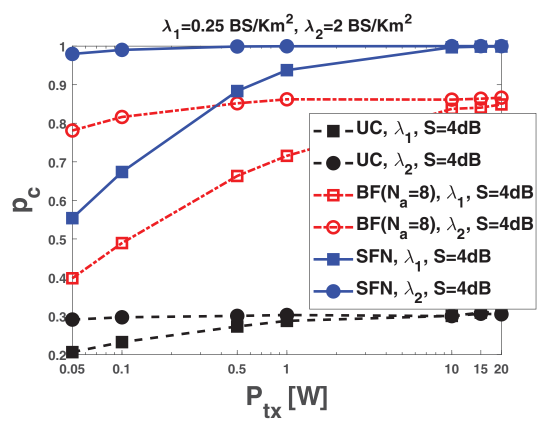

Figure 2. Coverage probability p_c in UC, BF, and SFN modes as a function of P_{tx}, with $N_a = 8$, $S = 4\ dB$, and two BS density values ($\lambda_1 = 0.25\ BS/km^2$ and $\lambda_2 = 2\ BS/km^2$).

broadcast mode (SFN), stands out as a robust solution for disseminating critical information. Our results convincingly demonstrate that these modes significantly outperform the UC transmission mode. However, our main contribution lies in identifying threshold parameters, which define the levels beyond which the relative efficiency in terms of coverage probability switches between BF and SFN modes. The focus on optimizing and predicting user coverage in UC, BF, and SFN modes, as well as finding an optimal trade-off between coverage and key system parameters, pave the way for smarter, more efficient 5G network planning. This study proposes practical solutions for managing security risks in densely populated areas, reinforcing the robustness of communication networks in the face of saturation. It represents a fundamental step forward in implementing communication systems to more secure and robust environments by judiciously choosing the optimum transmission mode among UC, BF, and SFN.

6. References

1. R. Borralho, A. Mohamed, A. U. Quddus, P. Vieira, and R. Tafazolli, "A Survey on Coverage Enhancement in Cellular Networks: Challenges and Solutions for Future Deployments," *IEEE Communications Surveys & Tutorials*, **23**, 2, January 2021, pp. 1302-1341.
2. M. Younes and Y. Louet, "Optimization of the Tradeoff Between Spectral Efficiency and Energy Efficiency in the Sub-Terahertz Context," Fifth IEEE International Workshop on Mobile Terahertz Systems (IEEE IWMTS), Duisburg, Germany, July 4–6, 2022, pp. 1-4.
3. M. Kamel, W. Hamouda, and A. Youssef, "Ultra-Dense Networks: A Survey," *IEEE Communications Surveys & Tutorials*, **18**, no. 4, May 2016, pp. 2522-2545.
4. M. Younes and Y. Louet, "Analysis of Unicast/Broadcast Switch over with Regard to Resource Allocation for Future Cellular Networks," 4th IEEE Global Power, Energy and Communication Conference (IEEE GPECOM), Cappadocia, Turkey, June 2022, pp. 605-610.
5. I. Ahmed, H. Khammari, A. Shahid, et al., "A Survey on Hybrid Beamforming Techniques in 5G: Architecture and System Model Perspectives," *IEEE Communications Surveys & Tutorials*, **20**, 4, June 2018, pp. 3060-3097.
6. A. N. Uwaechia and N. M. Mahyuddin, "A Comprehensive Survey on Millimeter Wave Communications for Fifth-Generation Wireless Networks: Feasibility and Challenges," *IEEE Access*, **8**, March 2020, pp. 62367-62414.
7. E. Pateromichelakis, M. Shariat, A. U. Quddus, and R. Tafazolli, "On the evolution of multi-cell scheduling in 3GPP LTE/LTE-A," *IEEE Communications Surveys & Tutorials*, **15**, 2, 2013, pp. 701–717.
8. M. Younes and Y. Louet, "Optimal Density of Base Stations in Dense Networks from the Point of View of Energy Efficiency," *URSI Radio Science Letters*, **4**, June 2022, pp. 1-5.
9. C. Diouf, M. Younes, A. Noaja, et al., "Robustness Analysis of a Parallel Two-Boxes Digital Polynomial Predistorter for an SOA-Based CO-OFDM System," *Optics Communications*, **402**, 1, November 2017, pp. 442-452.
10. M. Younes, M. Telescu, N. Tanguy, C. Diouf, P. Morel, and S. Azou, "Robustness Improvement of Compact Predistorters in a CO-OFDM System Using Semiconductor Optical Amplifiers," 29th IEEE International Conference on Microelectronics (IEEE ICM), Beirut, Lebanon, December 10–13, 2017, pp. 1-4.
11. J. E. Sime, P. Morel, M. Younes, et al., "The Effects of Digital Predistortion in a CO-OFDM System—A Stochastic Approach," *IEEE Photonics Technology Letters*, **32**, 13, May 2020, pp. 763-766.
12. M. Younes and Y. Louet, "Optimizing 5G Performance in Security Threat Situations: A Question of Coverage and Modeling," XXXVth General Assembly and Scientific Symposium of the International Union of Radio Science (URSI GASS), Sapporo, Japan, August 19–26, 2023, pp. 1-4.
13. 3GPP, TR 36.942, *Evolved Universal Terrestrial Radio Access (E-UTRA); Radio Frequency (RF) System Scenarios*, version 15.0.0, 3GPP, Washington, DC, July 2018.
14. T. T. Vu, L. Decreusefond, and P. Martins, "An Analytical Model for Evaluating Outage and Handover Probability of Cellular Wireless Networks," *Wireless Personal Communications*, **74**, January 2014, pp. 1117-1127.